Influence of pulse line switch inductance on output characteristics of high-current nanosecond accelerators

A I Mashchenko and I I Vintizenko
Institute of Physics and Technology, Tomsk polytechnic university, av. Lenina 30, Tomsk, 634050, Russia

E-mail: vintizenko@tpu.ru

Abstract. Various types of high-current nanosecond accelerators are simulated numerically using an equivalent circuit representation. The influence of pulse forming line switch inductance on the amplitude and waveform of output voltage and current pulses is analyzed.

1. Introduction

High-current (kiloampere level) nanosecond accelerators of charged particles [1] have a typical electrical scheme containing a pulse forming line (PFL), its switch, and charging unit. For PFL charging, various pulsed power supplies, Marx generators, or magnetic pulse generators are employed. Different types of PFL are possible: single line, double (Blumlein) line, in planar or coaxial geometry. Magnetic switches or spark gaps are used for PFL switching. For linear induction accelerators (LIAs) [2, 3], a set of ferromagnetic core inductors for voltage adding is included between a PFL and a load; there are also schemes with a high-voltage transformer [4].

It is implied that the inductance of the PFL switch and connections should be minimal to obtain the output pulse duration corresponding to the PFL electric length. The mentioned inductance, along with the PFL capacitance, determines the output pulse amplitude, full width, and rise-time. To reduce the inductance, multichannel spark gaps, spark gaps with small cathode-anode distance operating at a high gas pressure, or magnetic switches in the form of saturation chokes with single-turn windings and ferromagnetic cores having a rectangular hysteresis loop are employed. An analytical calculation of the inductance of the switch and connections is not always possible, so that such an important parameter usually is not indicated in the literature on the high-current nanosecond accelerators development. The analysis of the influence of PFL switch inductance on the amplitude and the waveform of the output pulses is possible using an equivalent circuit of the accelerator.

2. Equivalent circuit

The equivalent electric scheme of the accelerators is presented in figure 1. Its main elements are the power supply source PS, the double forming line DFL, the switch K, the high-voltage transformer T (ferromagnetic induction system if the LIA is simulated) and the ohmic load R_L. The scheme of the accelerator with the single PFL is obtained by excluding the cells of the second DFL section. Excluding the elements of the high-voltage transformer, one can reduce the scheme to that of usual accelerator, in which the PFL is directly connected to the load.

The following assumptions are accepted in the scheme: the distributed capacitances of the high-voltage transformer (induction system) and the load are replaced with the lumped ones; the line DFL is uniform (characteristic impedance is constant); ohmic losses and leakages in the line are neglected; the magnetization inductance of the transformer is a linear parameter; the electron diode, as the load, is replaced with the ohmic resistance.

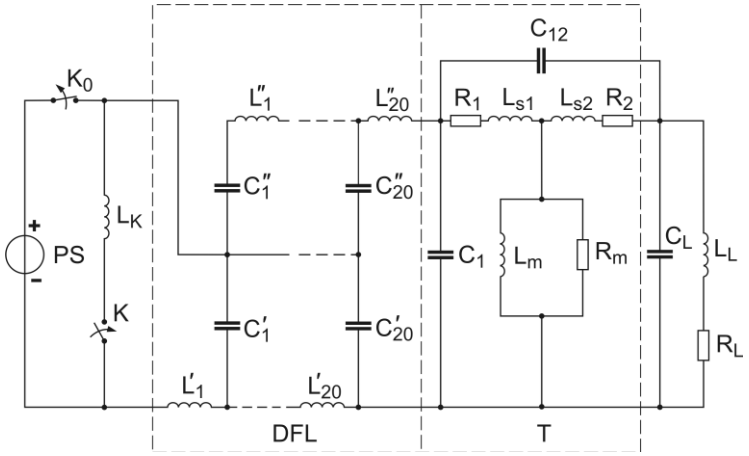

Figure 1. The equivalent electric scheme of accelerators.

The elements of the scheme are the following. L_K is the switch inductance, $L_1^{'} - L_{20}^{'}$, $L_1^{''} - L_{20}^{''}$, $C_1^{'} - C_{20}^{'}$, and $C_1^{''} - C_{20}^{''}$ are the inductances and capacitances per cell of the DFL sections. L_{S1}, L_{S2}, R_1, and R_2 are the leakage inductances and resistances of the transformer primary and secondary windings, respectively, L_m is the magnetization inductance of the transformer, R_m stands for the ohmic equivalent of losses in the transformer core, C_1 and C_{12} are, respectively, the input capacitance of the transformer and dynamic capacitance between its primary and secondary windings. C_L and L_L are the dynamic capacitance and the inductance of the load.

The resistances, inductances and capacitances per cell of the line, and dynamic capacitances and inductances can be easily calculated analytically using well-known expressions. For estimating the value of L_m, we use the theory of pulsed remagnetization of the ferromagnetic core [3]. The magnetization inductance L_m reflects the process of the transformer core magnetizing during discharging the PFL. The losses of energy in the core are determined as follows:

$$W_m = VH_0\Delta B + \frac{2VB_s}{\tau}\left(S_{\omega o}\lambda^2 + S_{\omega e}\lambda^3\right), \quad (1)$$

where V is the volume of the core, H_0 is the starting field strength, ΔB is the induction increase in the core, B_s is the saturation induction, $S_{\omega o}$ is the index of switching due to eddy currents, $S_{\omega e}$ is the index of switching due to magnetic viscosity, and $\lambda = \Delta B/2B_s$ is the index of the core loading by the flux linkage.

We determine the value of the magnetization inductance from the flux linkage of the transformer ψ_m:

$$L_m = \frac{\Psi_m}{\Delta I_m}, \quad (2)$$

where ΔI_m is the magnetization current. $\psi_m = lB_S k\omega(D_T - d_T)n$ where l is the width of the core steel, n is the number of cores, ω is the number of magnetization turns, $k \approx 0.8$ is the steel filling coefficient of the core for permalloy 50 NP (50% Fe, 50% Ni, electron beam vacuum melting, 0.01 mm thickness of rolling), D_T and d_T are the outer and inner diameter of the core, respectively.

Using the expression for pulsed remagnetization of the steel (1) and assuming $\lambda = 1$ (full remagnetization of the core from $-B_S$ up to $+B_S$), it is possible to write:

$$\Delta I_m = \frac{\pi(D_T + d_T)[H_0\tau + 2S_{\omega e} + S_{\omega o}]n}{2\tau\omega}. \quad (3)$$

From (2) and (3), one can obtain:

$$L_m = \frac{2\omega^2 B_S lk\tau(D_T - d_T)}{\pi(D_T + d_T)[H_0\tau + 2S_{\omega e} + S_{\omega o}]n}. \quad (4)$$

The charging of the first DFL section occurs directly from the pulsed source PS, and the second DFL section is charged through the primary winding of the transformer T, whose core at this time is demagnetized to a condition opposite to an operational one, and the load R_L. The switch K is closed and the switch K_0 is opened when DFL is charged up to the maximal value. After that, the first DFL section is recharged and the first and second sections connected in series are discharged through the transformer forming the high-voltage pulse on the load.

3. Simulation results

For simulations, the ohmic load R_L = 60 Ohm was taken and DFL parameters of the operating accelerators were chosen. The PS voltage of 60 kV was taken for the accelerator with the transformer (with the factor n = 12); the usual accelerator was simulated for the PS voltage of 720 kV.

First, the accelerator Tonus-NT [5] was simulated, when DFL was discharged, without the transformer, directly to the load. The scheme of the accelerator includes the high-voltage transformer with resonant contours (Tesla transformer) charging the double forming line filled with the transformer oil and the high-voltage diode. The gas-filled trigatron spark gap with up to 10 atm operating pressure is used for the double forming line switching. The main accelerator parameters are as follows: accelerating voltage range 0.4–1 MeV, line impedance 36.6 Ω, pulse duration 60 ns, pulse repetition rate up to 10 pps.

The voltage and current pulses on the load at 0.7 nF capacitance and 620 nH inductance of one DFL section and varied inductance L_K are shown in figure 2.

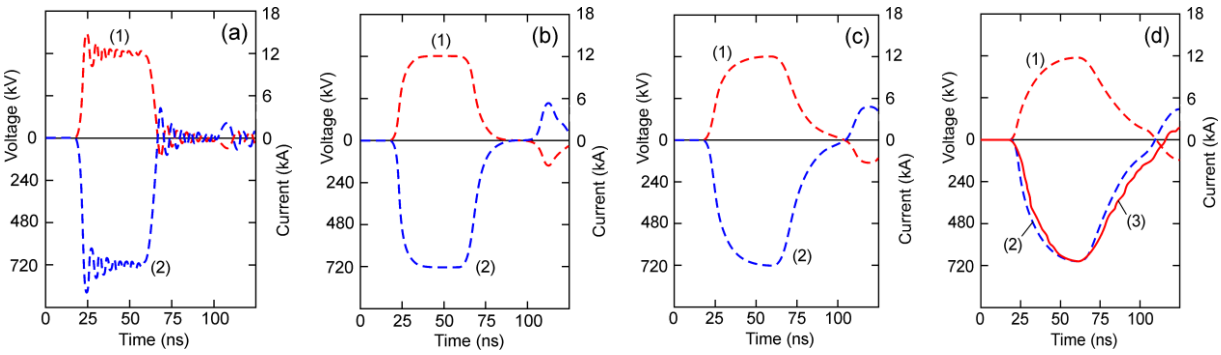

Figure 2. Simulated current (1) and voltage (2) pulses on the load R_L=60 Ohm. Inductance of the DFL switch: (a) L_K = 0 nH; (b) L_K = 100 nH; (c) L_K = 200 nH, (d) L_K = 320 nH. Tonus-NT observed voltage pulse (3).

The pulses have classical rectangular form (figures 2(a) and 2(b)) within a range of the switch inductance variation from 0 to 100 nH, the voltage value is U = 720 kV, the current is I = 12 kA and the duration is τ = 48 ns. At L_K = 200 nH, however, the rise and fall time of the pulses are lengthened, and their waveform becomes quasi-rectangular (figure 2(c)). The increase in the inductance L_K up to 320 nH (that corresponds to the inductance of the switch and connections in the Tonus-NT accelerator) results in more significant distortion of the pulse waveform, which approaches a trapezoidal one at U = 694 kV, I = 11.6 kA, and τ = 88 ns (figure 2(d)). The voltage reduction within the range of changing L_K from 0 up to 320 nH is small and caused by the increase in the pulse duration.

In the simulations of the full scheme of the accelerator (see figure 1) accounting for the parameters of the high-voltage transformer, the output pulses have a different waveform (figure 3). Even at L_K = 0 nH (figure 3(a)), the voltage and current pulses on the matched load have a triangular shape (simulations performed at 100 nF capacitance and 4.3 nH inductance of one DFL section). Such essential difference is due to the influence of the transformer, namely, the parasitic elements included to its equivalent circuit. The increase in the switch inductance from 5 nH (figure 3(b)) up to 18 nH (figure 3(d)) changes only the amplitude and duration of the pulses but not their waveform.

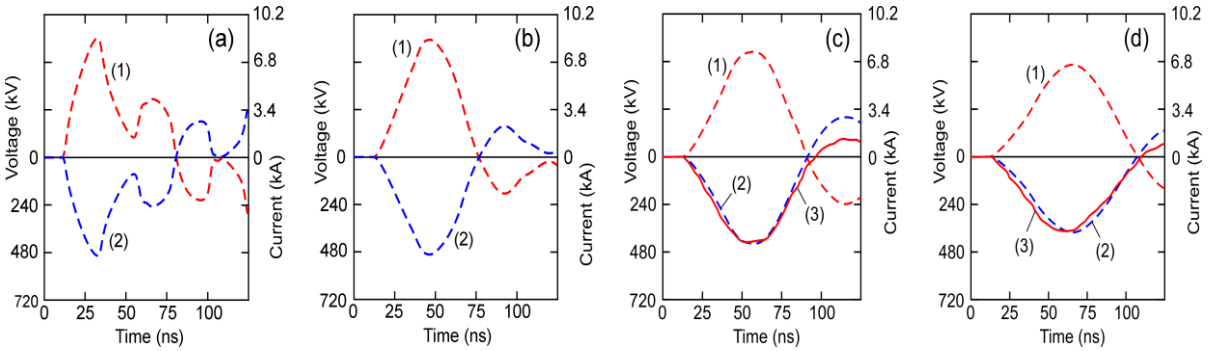

Figure 3. Simulated current (1) and voltage (2) pulses on the load R_L = 60 Ohm (R'_L = 0.416 Ohm reduced to the primary circuit) from the simulations of the scheme including the high-voltage transformer. The inductance of the DFL switch L_K is: (a) – 0 nH; (b) – 5 nH; (c) – 10 nH; (d) – 18 nH. LIA observed voltage pulses (3).

The amplitudes of the output voltage and current are following: at L_K = 5 nH, U = 495 kV, I = 8.26 kA, τ = 125 ns; at L_K = 10 nH, U = 439 kV, I = 7.32 kA, τ = 155 ns; at L_K = 18 nH, U = 405 kV, I = 6.75 kA, τ = 175 ns. Thus, the increase in the switch inductance from 0 up to 18 nH leads to the decrease in the accelerator output pulse power by ~34%; the pulse duration increases by ~11%.

Comparing the amplitudes and waveforms of the simulated pulses with the observed pulses of the accelerators Tonus-NT and LIA at Tomsk Polytechnic University, one can note the following. The difference in the amplitude and the duration of the simulated and observed pulses does not exceed 5%. The absence of the high-voltage transformer in the design of Tonus-NT allows forming the pulse trapezoidal on the load, even at the inductance of discharging contour as high as 320 nH.

The LIA with the multichannel spark gap has ~10 nH inductance of discharging contour (figure 3(c)) despite of multichannel switching (24 channels), synchronization of triggering the channels and forced division of current between the channels. The value of inductance is determined by the connections between the switch, DFL electrodes, and the induction system.

The LIA with the magnetic switch [6] has ~18 nH inductance of discharging contour (figure 3(d)). The higher inductance is caused by the processes of pulsed remagnetization of the switch cores, as the connections to the DFL and induction system is the same as for the LIA with spark gap switching. Thus, to decrease the inductance of discharging contour in the LIA with magnetic switching, one needs a core material with magnetization characteristics better than those of permalloy 50 NP.

However, common disadvantage of the accelerators with the transformer in the output circuit (the LIA is related to) is connected with the presence of parasitic reactive elements essentially affecting the output characteristics.

4. Conclusion

As a result of elaboration of the model including an analytical calculation of the circuit elements, a good agreement between the simulated pulses and the observed pulses of the working nanosecond accelerator (figure 2(d)) and linear induction accelerators (figures 3(c) and 3(d)) was achieved. It allows one to use the mentioned simulation model for the analysis of the influence of the element parameters of the equivalent circuit (in particular, PFL switch inductance changing in a wide range) on the amplitude and the waveform of the accelerator pulses on a load.

For the nanosecond accelerators decreasing inductance of the PFL switch and connections from 320 nH (Tonus-NT) down to 200 nH and below facilitates the formation of close-to-rectangular pulses. At the same time, within the 0–320 nH range of the switch inductance variation, the output pulse waveform depends on L_k significantly, and the amplitude changes slightly. Another situation takes place for the linear induction accelerators, with the spark gaps or with the magnetic commutators. Even the switch inductance and connections as low as several nH does not allow one to form a quasi-rectangular pulse; it looks rather triangular in accordance with simulations. With increasing inductance of the switch from 0 to 18 nH, the amplitude of the output pulse decreases and the pulse duration rises significantly but the waveform does not change. Such a difference between nanosecond accelerators and LIAs is connected with the presence of the induction system (high-voltage transformer) in LIAs; the elements of its equivalent circuit (dynamic capacitances, leakage and magnetization inductances, ohmic equivalents of losses in windings and magnetic system) determine the waveform and amplitude of the output pulses. The simulation has shown that the leakage inductance L_{S1} exerts the greatest influence. Therefore, for such accelerators, special attention must be devoted to designing the induction system (high-voltage transformer) and to a choice of the ferromagnetic core material (the parameters H_0, $S_{\omega o}$, $S_{\omega e}$) in order to achieve the maximal value of the magnetization inductance L_m. The simulation based on the presented equivalent circuit allows one to predict the characteristics of the output pulses of high-current nanosecond accelerators to a sufficient accuracy (~ 5%) and can be used for preliminary development of various types of accelerators with spark gaps, magnetic switches, Blumlein and single PFLs, with high-voltage transformers (induction systems) and without them in a discharging contour.

References

[1] Humphries S 2013 *Charged particle beams* (New York: Dover edition)
[2] Takayma K and Briggs R J 2011 *Induction accelerators* (New York: Springer science and business media)
[3] Vintizenko I I 2015 *Linear induction accelerator* (Moscow: Fizmatlit)
[4] Mazarakis M G et al 2010 *IEEE Transactions on Plasma Science* **38** 704
[5] Ryabchikov A I, Petrov A V, Karpov V B, Polkovnikova N M, Tolmacheva V G and Usov Yu P 2001 *Proceedings of the 5th Korea-Russia International Symposium on Science and Technology, (Tomsk)* vol 1 (Tomsk: TPU), pp372-375
[6] Chandra R et al 2014 *IEEE Transactions on Plasma Science* **42** 3491